Pharmacological potential of 3-((indol-3-yl)methyl)-6-methyl-[1,2,4]triazolo[3,4-b][1,3,4]thiadiazine-7-carbohydrazide and its N′-arylidene carbohydrazides

S. O. Fedotov[A–D], A. S. Hotsulia[E,F]

Zaporizhzhia State Medical and Pharmaceutical University, Ukraine

A – research concept and design; B – collection and/or assembly of data; C – data analysis and interpretation; D – writing the article; E – critical revision of the article; F – final approval of the article

Rational design of novel biologically active compounds relies on the use of effective structural fragments capable of providing high bioaffinity, favorable pharmacokinetic properties, and an adequate safety profile. Among them, scaffolds based on 1,2,4-triazole and indole occupy a special place; they are widely represented in pharmacologically active molecules due to their ability to participate in diverse types of molecular interactions.

Combining 1,2,4-triazole and indole fragments within a single molecule promotes the formation of conjugated systems with potentially multifunctional activity, thereby expanding opportunities for the development of new therapeutic agents. Computer-aided prediction of toxicological and pharmacokinetic properties at early stages of development remains a key strategy for optimizing screening. The use of *in silico* methods enables timely assessment of safety, the ADME profile and biological potential prior to experimental studies.

The aim of the study was an *in silico* evaluation of ADME parameters and molecular docking results for 3-((indol-3-yl)methyl)-6-methyl-[1,2,4]triazolo[3,4-*b*][1,3,4]thiadiazine-7-carbohydrazide and its *N′*-arylidene carbohydrazide derivatives, to substantiate the feasibility of their synthesis and further experimental investigations.

Materials and methods. The study was performed using computational methods. Drug-likeness and pharmacokinetic parameters were calculated with the SwissADME online platform. Molecular docking was carried out using AutoDock Vina and Discovery Studio Visualizer, applying the optimal parameters of the docking grid and analysis of interactions between the ligands and active sites of the target proteins. The following targets were selected: lanosterol 14α-demethylase (CYP51, PDB: 5V5Z), cyclooxygenase-2 (COX-2, PDB: 5IKR), peptide deformylase from *Staphylococcus aureus* (PDF, PDB: 1Q1Y), peptide deformylase from *Escherichia coli* (PDF, PDB: 1G2A), and anaplastic lymphoma kinase (ALK, PDB: 2XP2).

Results. The studied compounds have a high proportion of aromatic fragments and low saturation, accompanied by variable solubility and a generally acceptable drug-likeness profile. Molecular docking revealed target-specific lead compounds. The highest stability of COX-2 complexes was predicted for compounds 4 and 6 (ΔG = -10.2 kcal/mol). Compound 5 demonstrated the strongest binding to lanosterol 14α-demethylase with a binding energy of -11.0 kcal/mol. For peptide deformylase from *S. aureus*, compound 6 showed the most favorable interaction (ΔG = -8.4 kcal/mol), whereas compounds 7 and 9 were identified as the best binders to *E. coli* peptide deformylase (ΔG = -7.1 kcal/mol). In the case of ALK, compound 8 exhibited the highest binding affinity (ΔG = -9.0 kcal/mol).

Conclusions. The analyzed compounds may be considered as promising scaffolds for further *in vitro* and *in vivo* studies, particularly as potential multitarget pharmacological agents. The most relevant candidates for experimental validation are compounds 2, 5–8 and 10, as they combine a favorable pharmacokinetic balance with high predicted binding affinity toward several biological targets.

Key words: 1,2,4-triazole, indole, carbohydrazide, N′-arylidene carbohydrazides, SwissADME, molecular docking.

Current issues in pharmacy and medicine: science and practice. 2026;19(1):18-27

Фармакологічний потенціал 3-((індол-3-іл)метил)-6-метил-[1,2,4]тріазоло[3,4-b][1,3,4]тіадіазин-7-карбогідразиду та його N′-ариліденкарбогідразидів

С. О. Федотов, А. С. Гоцуля

Раціональний дизайн нових біологічно активних сполук спирається на використання ефективних структурних фрагментів, що можуть забезпечити високу біоафінність, сприятливі фармакокінетичні властивості й адекватний профіль безпеки. Серед них особливе значення мають каркаси на основі 1,2,4-тріазолу та індолу; вони широко представлені у фармакологічно активних молекулах завдяки здатності брати участь у різноманітних типах молекулярних взаємодій.

ARTICLE INFO

UDC 615.31:547.792.9:547.759:004.942
DOI: 10.14739/2409-2932.2026.1.351413

Current issues in pharmacy and medicine: science and practice. 2026;19(1):18-27

Keywords: 1,2,4-triazole, indole, carbohydrazide, N′-arylidene carbohydrazides, SwissADME, molecular docking.

Received: 10.11.2025 // Revised: 22.12.2025 // Accepted: 08.01.2026

З'єднання фрагментів 1,2,4-тріазолу та нижче в межах окремих молекул сприяє утворенню кон'югованої системи з проявом багатофункціональної активності, тим самим розширюючи можливості для розробки нових терапевтичних засобів. Комп'ютерне прогнозування токсикологічних і фармакокінетичних властивостей на ранніх стадіях розробки залишається ключовою стратегією для оптимізації скринінгу. Використання методів *in silico* дає змогу легко оцінити безпеку, профіль ADME та біологічний потенціал до здійснення експериментальних досліджень.

Мета роботи – *in silico* оцінювання параметрів ADME та результатів молекулярного докінгу для 3-((індол-3-іл)метил)-6-метил-[1,2,4]тріазоло[3,4-b][1,3,4]тіадіазин-7-карбогідразиду та його N′-ариліденкарбогідразидних похідних для обґрунтування можливості їх синтезу та подальших експериментальних досліджень.

Матеріали і методи. Дослідження здійснили, застосувавши обчислювальні методи. Параметри лікарської подібності та фармакокінетики розраховували за допомогою онлайн-платформи SwissADME. Молекулярний докінг здійснили за допомогою AutoDock Vina та Discovery Studio Visualizer, використали оптимальні параметри докінгової сітки та проаналізували взаємодії між лігандами й активними центрами цільових білків. Обрано такі мішені, як ланостерол 14α-деметилаза (CYP51, PDB: 5V5Z), циклооксигеназа-2 (COX-2, PDB: 5IKR), пептиддеформілаза з *Staphylococcus aureus* (PDF, PDB: 1Q1Y), пептиддеформілаза з *Escherichia coli* (PDF, PDB: 1G2A) та кіназа анапластичної лімфоми (ALK, PDB: 2XP2).

Результати. Досліджені сполуки характеризуються високою часткою ароматичних фрагментів і низькою насиченістю, що супроводжується змінною розчинністю та загалом прийнятним профілем лікарської подібності. Молекулярний докінг показав специфічні для мішеней провідні сполуки. Найвищу стабільність комплексів COX-2 передбачено для сполук 4 і 6 (ΔG = -10,2 ккал/моль). Сполука 5 мала найсильніше зв'язування з ланостерол 14α-деметилазою з енергією зв'язування -11,0 ккал/моль. Для пептидної деформілази *S. aureus* сполука 6 показала найсприятливішу взаємодію (ΔG = -8,4 ккал/моль), а сполуки 7 та 9 визначено як найкращі зв'язувальні речовини для пептидної деформілази *E. coli* (ΔG = -7,1 ккал/моль). Щодо ALK сполука 8 показала найвищу спорідненість зв'язування (ΔG = -9,0 ккал/моль).

Висновки. Проаналізовані сполуки визначено як перспективні каркаси для подальших досліджень *in vitro* та *in vivo*, зокрема як потенційні багатоцільові фармакологічні агенти. Найбільш релевантними кандидатами для експериментальної валідації є сполуки 2, 5–8 і 10, оскільки вони поєднують сприятливий фармакокінетичний баланс із високою прогнозованою спорідненістю зв'язування з кількома біологічними мішенями.

Ключові слова: 1,2,4-тріазол, індол, карбогідразид, N′-ариліденкарбогідразиди, SwissADME, молекулярний докінг.

Актуальні питання фармацевтичної і медичної науки та практики. 2026. Т. 19, № 1(50). С. 18-27

Development of new heterocyclic compounds remains one of the key directions of modern medicinal chemistry [1,2]. Indole fragments, owing to their structural diversity and considerable biological potential, occupy an important place among privileged scaffolds of bioactive molecules [3,4]. In parallel, the 1,2,4-triazole core promotes a broad spectrum of pharmacological activities, including antimicrobial, antifungal, and hypoglycemic effects, while maintaining a favorable safety profile, which underpins its value in the development of new therapeutic agents [5,6,7].

The concept of molecular hybridization, which involves the rational combination of bioactive fragments within a single molecule, is a promising strategy for creating compounds with enhanced efficiency and broadened action mechanisms [8,9,10]. In this context, conjugation of indole and 1,2,4-triazole fragments is expected to reveal new structures capable of interacting with various biological targets, including enzymes involved in inflammatory responses, microbial metabolism and signal transduction pathways [11,12].

Given the growing demand for new agents with improved pharmacokinetic properties and lower toxicity, *in silico* methods are increasingly used for early screening and prioritization of lead compounds. Prediction of absorption, distribution, metabolism, and excretion (ADME) parameters, along with molecular docking, enables identification of the most promising candidates for subsequent synthesis and biological testing.

Aim

The aim of the study was an *in silico* evaluation of ADME parameters and molecular docking results for 3-((indol-3-yl)methyl)-6-methyl-[1,2,4]triazolo[3,4-*b*][1,3,4]thiadiazine-7-carbohydrazide and its *N′*-arylidene carbohydrazide derivatives, to substantiate the feasibility of their synthesis and further experimental investigations.

Materials and methods

The virtual library of compounds for *in silico* studies was generated based on analysis of published data of biologically active structures containing indole and 1,2,4-triazole fragments, and by considering key principles of organic chemistry. This approach enabled rational integration of pharmacophoric fragments and ensured structural diversity of the designed molecules.

The studied series includes the structures shown in *Fig. 1*. Compound **1** is 3-((indol-3-yl)methyl)-6-methyl-[1,2,4]triazolo[3,4-*b*][1,3,4]thiadiazine-7-carbohydrazide. Compounds **2**–**10** are the corresponding *N′*-arylidene carbohydrazides that differ in the aryl fragment.

Analysis of physicochemical properties and prediction of bioavailability and pharmacokinetic parameters were performed using the SwissADME online platform.

Molecular docking was performed using AutoDock Vina and Discovery Studio Visualizer [13,14,15]. Energy minimization of ligands and preparation of the protein structures were carried out according to standard protocols. Docking grids were centered on the active sites of the target proteins with dimensions sufficient to cover the binding pockets. Binding modes were analyzed by calculating binding free energies (ΔG) and identifying key intermolecular interactions between the ligands and amino acid residues.

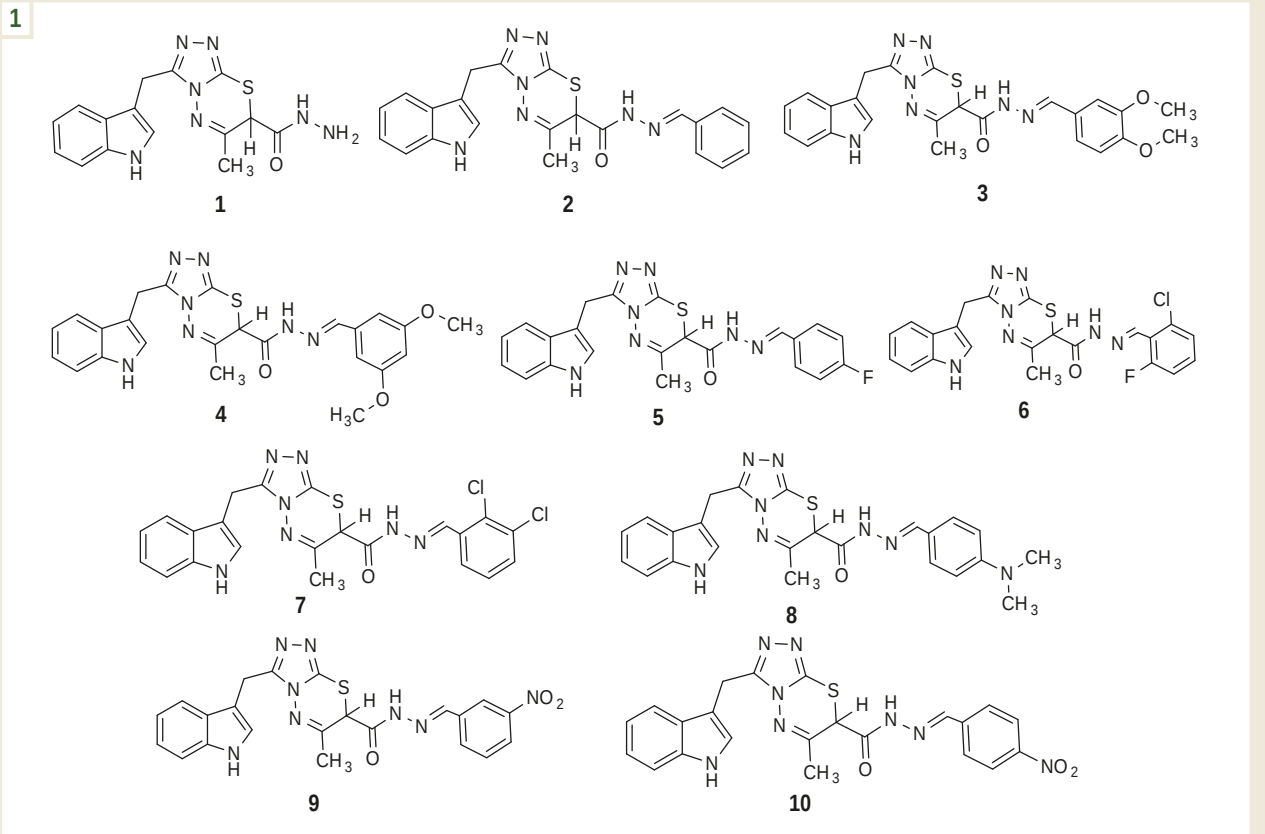

Fig. 1. Structure of the selected compounds for *in silico* studies.

Results

According to the bioavailability radar, the investigated molecules generally comply with the "drug-like" profile and can be considered as starting structures for further optimization. The SIZE parameter lies within the optimal range: molecular weight is 341.39–498.39 g/mol. Flexibility (FLEX) is moderate, with 4–8 rotatable bonds. Lipophilicity (XlogP3) ranges from 1.14 (**1**) to 4.78 (**7**) and approaches the upper limit for compounds **6** and **7**. The most pronounced deviations concern POLAR and SATU: for compounds **1**–**4** and **9**–**10,** TPSA exceeds 130 Å^2 (139.28–171.44 Å^2), whereas for **2** and **5**–**8** TPSA falls within the optimal zone or close to the upper limit (125.62–128.86 Å^2). For the entire series, SATU is outside the recommended interval due to the low Csp^3 fraction (0.14–0.21), indicating a predominantly aromatic character. According to the INSOLU (ESOL) parameter, the best solubility is predicted for compound **1** (logS = -2.84), whereas for most other derivatives logS corresponds to low solubility (approximately -4.80 to -5.99).

The molecular weight (MW) of the compounds does not exceed 500 g/mol, which is consistent with basic criteria for oral drug-likeness. The number of heavy atoms is 24–35, including 14–20 aromatic heavy atoms, indicating sufficient structural complexity and a high degree of aromaticity *(Table 1)*. The Csp^3 fraction, which indirectly characterizes saturation and three-dimensionality, is 0.14–0.21. This is below desirable values and may be one factor contributing to reduced aqueous solubility and passive permeability *(Table 1)*. The number of rotatable bonds is 4–8, i. e., within the range usually considered acceptable for drug-like molecules (≤9). Thus, the flexibility of the studied derivatives is moderate and should not markedly limit oral bioavailability due to entropic penalties. According to Lipinski's rule, the number of hydrogen-bond acceptors (HBA) should not exceed 10 and donors (HBD) should not exceed 5. For the studied amides, HBA is 5–7 and HBD is 2–3, which is favorable for specific intermolecular interactions. The molar refractivity (MR) (94.53–137.79) and the topological polar surface area (tPSA) (125.62–171.44 Å^2) additionally reflect steric and polar properties relevant to distribution in media of different polarity and transport across membranes *(Table 1)*.

Prediction of water solubility using three models (ESOL, Ali and SILICOS-IT) shows both substantial variability between compounds and model dependence. According to ESOL, logS ranges from -2.84 to -5.99 (approximately 4.91×10^{-1} to 5.05×10^{-4} mg/mL), whereas the Ali model yields more conservative values of -3.66 to -7.15 (approximately 7.49×10^{-2} to 3.53×10^{-5} mg/mL), and SILICOS-IT gives -4.30 to -8.36 (approximately 1.69×10^{-2} to 2.16×10^{-6} mg/mL). Discrepancies between algorithms are expected because they account differently for the contributions of lipophilicity, polarity, and structural complexity *(Table 2)*.

Compound **1** consistently shows the highest predicted water solubility (logS: -2.84 by ESOL; -3.66 by Ali; -4.30 by

Table 1. Physicochemical properties of the studied compounds

Parameter	1	2	3	4	5	6	7	8	9	10
MW, g/mol	341.39	429.50	489.55	489.55	447.49	481.93	498.39	472.57	474.50	474.50
Heavy atoms	24	31	35	35	32	33	33	34	34	34
Aromatic heavy atoms	14	20	20	20	20	20	20	20	20	20
Csp^3 fraction	0.20	0.14	0.21	0.21	0.14	0.14	0.14	0.21	0.14	0.14
Rotatable bonds	4	6	8	8	6	6	6	7	7	7
H-bond acceptors (HBA)	5	5	7	7	6	6	5	5	7	7
H-bond donors (HBD)	3	2	2	2	2	2	2	2	2	2
MR	94.53	124.81	137.79	137.79	124.76	129.77	134.83	139.01	133.63	133.63
tPSA, $Å^2$	139.28	125.62	144.08	144.08	125.62	125.62	125.62	128.86	171.44	171.44

Table 2. Water solubility of the studied compounds

Parameter	1	2	3	4	5	6	7	8	9	10
Log S (ESOL)	-2.84	-4.80	-4.96	-4.96	-4.96	-5.56	-5.99	-5.04	-4.87	-4.87
Solubility										
mg/mL	4.91×10^{-1}	6.78×10^{-3}	5.42×10^{-3}	5.42×10^{-3}	4.89×10^{-3}	1.33×10^{-3}	5.05×10^{-4}	4.28×10^{-3}	6.46×10^{-3}	6.46×10^{-3}
mol/L	1.44×10^{-3}	1.58×10^{-5}	1.11×10^{-5}	1.11×10^{-5}	1.09×10^{-5}	2.77×10^{-6}	1.01×10^{-6}	9.06×10^{-6}	1.36×10^{-5}	1.36×10^{-5}
Class	S	MS	MS	MS	MS	MS	MS	MS	MS	MS
Log S (Ali)	-3.66	-5.84	-6,18	-6,18	-5.95	-6.60	-7.15	-6.04	-6.63	-6.63
Solubility										
mg/mL	7.49×10^{-2}	6.18×10^{-4}	3.25×10^{-4}	3.25×10^{-4}	5.07×10^{-4}	1.21×10^{-4}	3.53×10^{-5}	4.26×10^{-4}	1.12×10^{-4}	1.12×10^{-4}
mol/L	2.19×10^{-4}	1.44×10^{-6}	6.64×10^{-7}	6.64×10^{-7}	1.13×10^{-6}	2.52×10^{-7}	7.09×10^{-8}	9.02×10^{-7}	2.36×10^{-7}	2.36×10^{-7}
Class	S	MS	PS	PS	MS	PS	PS	PS	PS	PS
Log S (SILICOS-IT)	-4.30	-7.20	-7.40	-7.40	-7.46	-8.04	-8.36	-7.27	-6.54	-6.54
Solubility										
mg/mL	1.69×10^{-2}	2.69×10^{-5}	1.96×10^{-5}	1.96×10^{-5}	1.53×10^{-5}	4.34×10^{-6}	2.16×10^{-6}	2.53×10^{-5}	1.38×10^{-4}	1.38×10^{-4}
mol/L	4.95×10^{-5}	6.27×10^{-8}	4.01×10^{-8}	4.01×10^{-8}	3.43×10^{-8}	9.02×10^{-9}	4.34×10^{-9}	5.36×10^{-8}	2.90×10^{-7}	2.90×10^{-7}
Class	MS	PS	PS	PS	PS	PS	PS	PS	PS	PS

S: soluble; **MS:** moderately soluble; **PS:** poorly soluble.

SILICOS-IT). For compound **2**, a pronounced model dependence is observed (approximately -4.0 to -7.2). Compounds **3** and **4** have similar values and are classified as poorly soluble by the Ali and SILICOS-IT models. Compound **5** remains within moderate solubility by ESOL and Ali; however, by SILICOS-IT the prediction decreases to -7.46. Among derivatives **6**–**10**, the lowest logS values are observed for compounds **7** (down to -8.36) and **6** (down to -8.04), whereas compounds **8–10** also exhibit low aqueous solubility *(Table 2)*.

Lipophilicity estimated by different algorithms (iLogP, XLogP3, WLogP, MLogP and SILICOS-IT) indicates predominantly moderate lipophilicity. By XLogP3, values range from 1.14 to 4.78, and the consensus logP is 1.23–4.19. Derivatives **6** and **7** are predicted to be the most lipophilic (XLogP3 4.73–4.78), which together with low solubility may limit absorption; the remaining compounds have values compatible with potential passive membrane diffusion *(Table 3)*.

According to SwissADME predictions, most compounds exhibit high gastrointestinal absorption (GI absorption) (**1**–**6**, **8**), whereas reduced absorption is expected for compounds **7**, **9** and **10** *(Table 4)*. For the entire series, blood-brain barrier (BBB) permeation is not predicted, indicating a low probability of central nervous system exposure *(Table 4)*. Compounds **1**, **3**, **4** and **8** are predicted to be substrates of P-glycoprotein (P-gp), which may reduce their intestinal absorption and/or promote efflux from cells, thereby affecting bioavailability *(Table 4)*. CYP inhibition profiles show potential interaction risks: compounds **1**, **2**, **5–7**, **9** and **10** may inhibit CYP isoforms (CYP1A2, CYP2C19, CYP2C9, CYP2D6, CYP3A4), which should be considered in further optimization and experimental evaluation *(Table 4)*. Skin permeation coefficients (Log Kp)

Table 3. Lipophilicity of the studied compounds

Parameter	1	2	3	4	5	6	7	8	9	10
Log Po/w (iLogP)	1.57	2.58	2.68	2.82	2.70	2.68	3.03	3.11	1.84	2.22
Log Po/w (XLogP3)	1.14	3.52	3.47	3.47	3.62	4.25	4.78	3.65	3.35	3.35
Log Po/w (WLogP)	0.66	2.82	2.84	2.84	3.38	4.03	4.12	2.88	2.73	2.73
Log Po/w (MLogP)	1.50	2.85	2.26	2.26	3.23	3.71	3.81	2.77	2.03	2.03
Log Po/w (SILICOS-IT)	1.28	3.91	4.05	4.05	4.33	4.98	5.20	3.61	1.76	1.76
Consensus Log Po/w	1.23	3.14	3.06	3.09	3.45	3.93	4.19	3.20	2.34	2.42

Table 4. Pharmacokinetics of the studied substances

Parameter	1	2	3	4	5	6	7	8	9	10
GI absorption	High	High	High	High	High	High	Low	High	Low	Low
BBB permeation	–	–	–	–	–	–	–	–	–	–
P-gp substrate	+	–	+	+	–	–	–	+	–	–
CYP1A2 inhibitor	+	+	–	–	+	+	+	–	–	–
CYP2C19 inhibitor	–	+	+	+	+	+	+	+	+	+
CYP2C9 inhibitor	–	+	+	+	+	+	+	+	+	+
CYP2D6 inhibitor	–	–	–	–	–	–	–	–	–	–
CYP3A4 inhibitor	–	+	+	+	+	+	+	+	+	+
Log Kp, cm/s	-7.57	-6.42	-6.82	-6.82	-6.46	-6.22	-5.95	-6.59	-6.82	-6.82

Table 5. Medicinal chemistry

Parameter	1	2	3	4	5	6	7	8	9	10
PAINS	+	+	+	+	+	+	+	+	+	+
Brenk filter	–	–	–	–	–	–	–	–	–	–
Lead-likeness	+	–	–	–	–	–	–	–	–	–
SA	4.10	4.56	4.80	4.81	4.54	4.57	4.56	4.80	4.65	4.62

range from -6.31 cm/s to -5.50 cm/s, which is consistent with limited transdermal penetration and suggests that topical delivery may require formulation enhancement *(Table 4)*.

None of the compounds contains PAINS structural alerts (0 violations), which reduces the risk of nonspecific activity in primary biochemical screening *Table 5*. Brenk filter analysis indicates the absence of unwanted substructures (0 alerts) for the entire series, supporting favorable medicinal chemistry characteristics *(Table 5)*. Lead-likeness assessment suggests that compounds **1** and **8** satisfy the criteria with no violations, whereas other derivatives show one or two deviations, primarily due to higher molecular weight and/or lipophilicity *(Table 5)*.

Synthetic accessibility (SA) values of 4.10–4.86 suggest moderate synthetic complexity and indicate that the designed structures are feasible for laboratory synthesis *(Table 5)*.

All studied compounds meet Lipinski's rule of five, which indicates the possibility of oral bioavailability. Therefore, no violations were identified for this filter *(Table 6)*. According to the Ghose filter, compounds **1**, **2**, **5–7** and **8** satisfy the criteria, whereas compounds **3**, **4**, **9** and **10** show one violation each, mainly due to excessive molar refractivity or lipophilicity *(Table 6)*. Veber filter analysis indicates that compounds **1**, **2**, **5**, **6–8** comply with the criteria, while compounds **3**, **4**, **9** and **10** fail due to elevated TPSA and the number of rotatable bonds *(Table 6)*. The Egan filter is passed by compounds **2**, **5–8**, whereas compounds **1**, **3**, **4**, **9** and **10** violate the criterion due to excessive polarity *(Table 6)*.

All compounds meet the Muegge filter requirements, which indicates overall acceptable drug-likeness of the series *(Table 6)*.

All investigated compounds (**1–10**) can bind to the active site of COX-2, forming stable complexes with binding free energies (ΔG) ranging from -8.7 kcal/mol to -10.2 kcal/mol. These values indicate potential inhibitory activity of the studied molecules toward COX-2.

The most energetically favorable were complexes of compounds **4** and **6** (ΔG = -10.2 kcal/mol). These ligands exhibit numerous stabilizing interactions, including hydrophobic and π-alkyl contacts with residues ALA A:528, VAL A:350 and

Table 6. Drug-likeness

Parameter	1	2	3	4	5	6	7	8	9	10
Lipinski filter	+	+	+	+	+	+	+	+	–	–
Ghose filter	+	+	–	–	+	–	–	–	–	–
Veber filter	+	+	–	–	+	+	+	+	–	–
Egan filter	–	+	–	–	+	+	+	+	–	–
Muegge filter	+	+	+	+	+	+	+	+	–	–
Bioavailability	0.55	0.55	0.55	0.55	0.55	0.55	0.55	0.55	0.55	0.55

LEU A:353, as well as aromatic interactions with GLY A:527 (amide-π stacking, T-shaped π-π contacts). For compound **6**, additional stabilization is provided by hydrogen bonds with TYR A:116 and SER A:120, a π-anion interaction with GLU A:525, and a halogen interaction with MET A:523, indicating an optimal orientation of the ligand within the enzyme active site *(Table 7)*.

High affinity to COX-2 was also shown by compounds **7** and **9** (ΔG = -10.1 kcal/mol). Their complexes are stabilized by a combination of hydrophobic contacts (ALA A:528, VAL A:350, VAL A:89, VAL A:117), amide-π and π-π interactions with GLY A:527, and hydrogen bonds with GLU A:525 and SER A:120. The residue TYR A:356 plays an important role in ligand anchoring, forming π-donor and π–S interactions typical of selective COX-2 inhibitor binding.

Compounds **2**, **3** and **5** have binding energies of -9.3 kcal/mol to -9.9 kcal/mol. Their binding is mediated mainly by multiple hydrophobic contacts with ALA A:528, VAL A:350 and LEU A:353, as well as aromatic interactions with GLY A:527 and, in some cases, PHE A:519. The presence of halogen bonds (Cl, F) in compound **5** may additionally enhance binding stability.

Compounds **1** and **10** (ΔG = -8.7 kcal/mol to -8.8 kcal/mol) exhibit the weakest binding within the series; however, they still form stable complexes supported by hydrophobic contacts with VAL A:350 and LEU A:353 and π-π interactions with TYR A:356, which suggests preservation of the general binding mode within the COX-2 pocket. Compound **8** (ΔG = -9.5 kcal/mol) forms a complex stabilized by hydrophobic interactions with ALA A:528, VAL A:350 and LEU A:353, as well as a hydrogen bond with GLU A:525 and aromatic interactions with GLY A:527, indicating a balanced interaction profile.

The entire series of structures (**1–10**) can form stable complexes with the active site of lanosterol 14α-demethylase, demonstrating high affinity with ΔG values in the range of -9.5 to -11.0 kcal/mol *(Table 8)*.

The most energetically favorable was the complex of compound **5** (ΔG = -11.0 kcal/mol). The stability of binding is driven by multiple hydrophobic interactions and π-alkyl contacts with residues LEU A:321, ALA A:256, MET A:509, LEU A:324 and ALA A:325, as well as by π-π stacking with PHE A:154. A key contribution is made by interactions with CYS A:394, which include π-alkyl contacts and conventional hydrogen bonds typical of azole-type inhibitors. High affinity was also predicted for compounds **7** and **10** (ΔG = -10.8 kcal/mol), which form stable complexes through a combination of hydrophobic interactions with LEU and ALA residues and aromatic contacts with PHE A:154 and TYR A:121. Compounds **2–4**, **6** and **9** have slightly higher ΔG values (-10.3 kcal/mol to -10.6 kcal/mol) but retain the key interaction pattern, including contacts with CYS A:394 and hydrophobic residues of the binding pocket. Compounds **1** and **8** show somewhat lower affinity (ΔG = -9.5 kcal/mol to -10.0 kcal/mol), yet still form stable complexes supported by interactions with CYS A:394, THR A:260 and hydrophobic amino acid residues, indicating preservation of the canonical binding mode in CYP51.

Thus, the docking results indicate that the designed *N′*-arylidene carbohydrazides can act as potential inhibitors of lanosterol 14α-demethylase and may serve as promising candidates for antifungal research, given their predicted high binding affinity and the presence of characteristic interactions in the active site of the enzyme.

The selected structures (**1–10**) can interact with the active site of peptide deformylase (PDF) from *S. aureus*, forming stable complexes with ΔG values in the range of -7.4 to -8.4 kcal/mol *(Table 9)*.

The most energetically favorable was the complex of compound **6** with PDF from *S. aureus* (ΔG = -8.4 kcal/mol). High stability is ensured by a combination of hydrogen bonds with SER A:57, TYR A:147 and GLY A:58, an electrostatic interaction with GLU A:185 (attractive charge), and a T-shaped π-π interaction with HIS A:154. Additional contributions come from hydrophobic π-alkyl contacts with VAL A:59, VAL A:151 and LEU A:112, indicating efficient occupation of the hydrophobic region of the enzyme active site. High affinity to PDF was also demonstrated by compounds **2**, **5**, **7** and **9** (ΔG = -8.0 kcal/mol to -8.2 kcal/mol). These molecules form multiple hydrogen bonds with ARG A:56, THR A:107, GLU A:155 and ASN A:117, as well as π-π and amide-π stacking interactions with HIS A:154 and GLY A:110, which play an important role in anchoring the ligands within the binding pocket. For compounds **5** and **9**, additional stabilization is provided by electrostatic interactions with GLU A:185, a characteristic feature of ligands capable of effective binding to the catalytic region of this enzyme.

Compounds **8** and **10** show similar binding energies (ΔG = -8.1 kcal/mol) and form complexes stabilized by intermolecular hydrogen bonds with SER A:57, HIS A:154 and HIS A:186, amide–π stacking interactions with GLY A:110,

Table 7. Molecular docking results for COX-2

Compound	ΔG, kcal/mol	Amino acid contacts (residues, interaction type)
1	-9.2	ALA A:528 (alkyl, π-alkyl); VAL A:350 (alkyl, π-alkyl); LEU A:353 (π-alkyl); GLY A:527 (amide-π stacking, π-π)
2	-9.9	ALA A:528 (alkyl, π-alkyl); VAL A:350 (alkyl, π-alkyl); LEU A:353 (π-alkyl); GLY A:527 (amide-π stacking; T-shaped π-π interaction)
3	-9.3	ALA A:528 (alkyl, π-alkyl); VAL A:350 (alkyl, π-alkyl); LEU A:353 (π-alkyl); GLY A:527 (amide stacking, π-π); PHE A:519 (π-π)
4	-10.2	ALA A:528 (alkyl, π-alkyl); VAL A:350 (alkyl, π-alkyl); LEU A:353 (π-alkyl); GLY A:527 (amide-π stacking); TYR A:356 (π–π); GLU A:525 (π-anion)
5	-9.7	ALA A:528 (alkyl, π-alkyl); VAL A:350 (alkyl, π-alkyl); LEU A:353 (π-alkyl); GLY A:527 (amide stacking, π-π); MET A:523 (halogen interaction, F)
6	-10.2	ALA A:528 (alkyl, π-alkyl); VAL A:350 (alkyl, π-alkyl); LEU A:353 (π-alkyl); GLY A:527 (amide-π stacking, T-shaped π-π); TYR A:356 (π-donor H-bond, π-S); SER A:120 (intermolecular H-bond)
7	-10.1	ALA A:528 (alkyl, π-alkyl); VAL A:350 (alkyl, π-alkyl); LEU A:353 (π-alkyl); GLY A:527 (amide stacking, π-π); GLU A:525 (H-bond); SER A:120 (intermolecular H-bond)
8	-8.7	ALA A:528 (alkyl, π-alkyl); VAL A:350 (alkyl, π-alkyl); LEU A:353 (π-alkyl); GLY A:527 (amide-π stacking); GLU A:525 (H-bond); SER A:120 (intermolecular H-bond, C–H bond); VAL A:89 (hydrophobic contacts)
9	-10.1	ALA A:528 (alkyl, π-alkyl); VAL A:350 (alkyl, π-alkyl); LEU A:353 (π-alkyl); GLY A:527 (amide-π stacking); GLU A:525 (H-bond); SER A:120 (H-bond); TYR A:356 (π–π)
10	-9.2	ALA A:528 (alkyl, π-alkyl); VAL A:350 (alkyl, π-alkyl); LEU A:353 (π-alkyl); GLY A:527 (amide-π stacking, π-π)

Table 8. Molecular docking results for lanosterol 14α-demethylase

Compound	ΔG, kcal/mol	Amino acid contacts (residues; interaction type)
1	-9.1	ARG A:96 (Alkyl, π-Alkyl), LEU A:321 (Alkyl, π-Alkyl), THR A:260 (π-σ), CYS A:394 (Alkyl, π-Alkyl), PRO A:320 (Alkyl, π-Alkyl), LEU A:324 (Alkyl, π-Alkyl), ALA A:400 (Alkyl, π-Alkyl), PHE A:387 (π-π T-shaped).
2	-10.3	LEU A:321 (π-Alkyl), TYR A:76 (π-π T-shaped), LEU A:100 (π-Alkyl), MET A:79 (π-Alkyl), ALA A:256 (π-σ), PHE A:78 (π-π T-shaped), LEU A:105 (π-Alkyl), PHE A:399 (π-π T-shaped), CYS A:394 (π-Alkyl).
3	-10.1	ALA A:104 (Alkyl, π-Alkyl), LEU A:105 (Alkyl, π-Alkyl), LEU A:152 (Alkyl, π-Alkyl), MET A:79 (Alkyl, π-Alkyl), GLY A:396 (C-H Bond), TYR A:76 (π-σ), ALA A:400 (Alkyl, π-Alkyl), ALA A:256 (π-σ), LEU A:100 (Alkyl, π-Alkyl), PHE A:399 (Alkyl, π-Alkyl), CYS A:394 (Conventional H Bond), PHE A:78 (π-π T-shaped), LEU A:321 (Alkyl, π-Alkyl)
4	-9.9	ARG A:96 (Alkyl, π-Alkyl), CYS A:394 (Conventional H Bond, π-Donor H Bond), LEU A:100 (Alkyl, π-Alkyl), MET A:79 (π-S), TYR A:76 (π-π Stacked, π-π T-shaped), VAL A:395 (Conventional H Bond), LEU A:321 (π-σ), ALA A:400 (Alkyl, π-Alkyl), PHE A:387 (Alkyl, π-Alkyl), PHE A:78 (π-π Stacked, π-π T-shaped).
5	-11.0	MET A:433 Halogen (F), LEU A:321 (Alkyl, π-Alkyl), PHE A:78 (π-π Stacked), GLY A:396 (π-σ), ARG A:96 (π-π Stacked), LEU A:100 (Alkyl, π-Alkyl), CYS A:394 (Conventional H Bond), ALA A:256 (π-S), LEU A:105 (Alkyl, π-Alkyl), LEU A:152 (Alkyl, π-Alkyl), PHE A:255 (π-σ)
6	-10.3	CYS A:394 (Conventional H Bond), GLY A:396 Halogen (F), MET A:79 (Alkyl, π-Alkyl), LEU A:105 (Alkyl, π-Alkyl), PHE A:78 (π-π Stacked), ALA A:256 (Alkyl, π-Alkyl), LEU A:100 (Alkyl, π-Alkyl), LEU A:321 (Alkyl, π-Alkyl)
7	-10.7	PHE A:399 (Alkyl, π-Alkyl), ALA A:256 (π-σ), LEU A:105 (Alkyl, π-Alkyl), LEU A:100 (Alkyl, π-Alkyl), TYR A:76 (π-π Stacked), MET A:79 (Alkyl, π-Alkyl), LEU A:152 (Alkyl, π-Alkyl), LEU A:321 (π-σ), PHE A:78 (π-π Stacked).
8	-10.6	LEU A:100 (π-Alkyl), ALA A:256 (π-σ), LEU A:105 (π-σ), HIS A:259 (C-H Bond), TYR A:76 (π-π T-shaped), LEU A:321 (π-Alkyl), ILE A:323 (C-H Bond), MET A:79 (π-Alkyl), PHE A:78 (π-π T-shaped), CYS A:394 (Conventional H Bond), PHE A:399 (π-π T-shaped), LEU A:152 (π-Alkyl)
9	-10.3	GLY A:257 (C-H Bond), ALA A:256 (π-σ), MET A:79 (π-Alkyl), LEU A:105 (π-Alkyl), LEU A:100 (π-Alkyl), PHE A:399 (π-π T-shaped), LEU A:321 (π-σ), PHE A:78 (π-π T-shaped), TYR A:76 (π-π T-shaped)
10	-10.8	MET A:433 (Conventional H Bond), ALA A:256 (π-σ), LEU A:100 (Alkyl, π-Alkyl), TYR A:76 (π-π T-shaped), LEU A:321 (Alkyl, π-Alkyl), PHE A:78 (π-π T-shaped), CYS A:394 (π-Sulfur), LEU A:105 (π-σ), ALA A:104 (Alkyl, π-Alkyl), ARG A:96 (Unfavorable Positive-Positive), MET A:79 (Alkyl, π-Alkyl), THR A:260 (Conventional H Bond), LEU A:152 (Alkyl, π-Alkyl)

and hydrophobic contacts with PRO A:78, VAL A:59, VAL A:151 and LEU A:112. For compound **8**, the largest number of diverse interactions was observed, indicating a well-adapted ligand conformation in the enzyme active site. Compounds **1**, **3** and **4** have slightly lower ΔG values (-7.4 kcal/mol to -7.9 kcal/mol). Their binding is mainly driven by hydrophobic π-σ and π-alkyl interactions with VAL A:59, VAL A:151 and LEU A:112, as well as T-shaped π-π contacts with HIS A:154. For compounds **1** and **3**, hydrogen bonds with ARG A:56 and GLU A:155 play an important role, whereas for compound **4** additional stabilization is provided by a hydrogen bond with TYR A:147.

Table 9. Molecular docking results for PDF from *S. aureus*

Compound	ΔG, kcal/mol	Amino acid contacts (residues; interaction type)
1	-7.8	VAL A:59 (π–σ); HIS A:154 (π–π T-shaped); ARG A:56 (H-bond); VAL A:151 (π-alkyl); LEU A:112 (π-alkyl)
2	-8.2	THR A:107 (π-donor H-bond); VAL A:59 (π–σ); HIS A:154 (π-donor H-bond; amide–π stacked; π–π T-shaped); GLY A:110 (amide–π stacked; π–π T-shaped); ARG A:56 (H-bond); VAL A:151 (π–σ); CSD A:111 (vdW); LEU A:112 (π-alkyl)
3	-7.4	GLU A:155 (H-bond); VAL A:59 (π–σ); HIS A:154 (π–π T-shaped); GLY A:58 (C–H bond); VAL A:151 (π–σ); ARG A:56 (H-bond); LEU A:112 (π-alkyl)
4	-7.9	PRO A:78 (alkyl; π-alkyl); TYR A:147 (H-bond); SER A:57 (C–H bond); GLN A:45 (C–H bond); HIS A:154 (π–π T-shaped); VAL A:59 (π–σ); VAL A:151 (alkyl; π-alkyl)
5	-8.2	PRO A:78 (π-alkyl); LEU A:112 (π-alkyl); GLY A:60 (unfavorable donor–donor); VAL A:59 (π-alkyl); TYR A:147 (C–H bond); ARG A:56 (attractive charge); HIS A:154 (π–π stacked); VAL A:151 (π-alkyl); GLU A:185 (π-cation)
6	-8.4	VAL A:59 (π-alkyl); HIS A:154 (π–π T-shaped); VAL A:151 (π–σ); SER A:57 (H-bond); TYR A:147 (H-bond); GLY A:58 (H-bond); GLU A:185 (attractive charge); LEU A:112 (π-alkyl)
7	-8.0	THR A:107 (π-donor H-bond); VAL A:59 (π-alkyl); GLU A:155 (H-bond); HIS A:154 (amide–π stacked; π–π T-shaped); GLY A:110 (amide–π stacked; π–π T-shaped); VAL A:151 (π–σ); ARG A:56 (H-bond); LEU A:112 (π-alkyl)
8	-8.1	PRO A:78 (alkyl; π-alkyl); HIS A:154 (π-donor H-bond; C–H bond); HIS A:186 (π-donor H-bond; C–H bond); VAL A:59 (alkyl; π-alkyl); SER A:57 (π-donor H-bond; C–H bond); GLU A:185 (attractive charge); GLY A:110 (amide-π stacked; π-π T-shaped); VAL A:151 (alkyl; π-alkyl); ARG A:56 (H-bond); LEU A:112 (alkyl; π-alkyl)
9	-8.2	GLU A:185 (attractive charge); VAL A:151 (π-alkyl); HIS A:154 (π–π stacked); GLU A:109 (π-anion); VAL A:59 (H-bond); ASN A:117 (π-donor H-bond)
10	-8.1	VAL A:59 (π–σ); VAL A:151 (π-alkyl); HIS A:154 (π–π stacked); SER A:57 (π-donor H-bond; C–H bond)

Table 10. Molecular docking results for PDF from *E. coli*

Compound	ΔG, kcal/mol	Amino acid contacts (residues; interaction type)
1	-6.5	GLU B:87 (Conventional H Bond); LEU B:91 (π-Alkyl, π-σ)
2	-6.7	ILE B:44 (π-σ); GLU B:95 (π-Anion); GLY B:89 (C–H Bond); ARG B:97 (Conventional H Bond)
3	-6.6	GLN B:96 (C–H Bond); ILE B:86 (π-Alkyl); ARG B:97 (π-Cation); LEU B:91 (π-Alkyl)
4	-6.5	GLU B:42 (C–H Bond); ILE B:86 (Alkyl, π-Alkyl); GLU B:88 (C–H Bond); GLY B:89 (Conventional H Bond); LEU B:91 (π-σ)
5	-6.5	ASP B:162 (Halogen bond, F); LEU B:161 (Halogen bond, F); GLU B:95 (Attractive charge); GLU B:41 (Attractive charge)
6	-6.8	GLU B:42 (Halogen bond, F); ARG B:97 (π-Cation); ILE B:86 (π-σ); LEU B:91 (Alkyl, π-Alkyl); ILE B:44 (Alkyl, π-Alkyl)
7	-7.1	ILE B:44 (Alkyl, π-Alkyl); PRO B:94 (Alkyl, π-Alkyl); GLY B:89 (Amide-π stacked; π-donor H bond); LEU B:161 (Alkyl, π-Alkyl); GLU B:95 (Attractive charge; π-Cation); ARG B:97 (Attractive charge; π-Cation)
8	-6.8	LEU B:91 (π-σ); ARG B:97 (π-Cation); LEU B:125 (π-σ); ILE B:86 (π-Alkyl)
9	-7.1	GLN B:96 (Conventional H Bond); ARG B:97 (π-Cation); ILE B:86 (π-Alkyl); LEU B:125 (π-Alkyl)
10	-6.6	ILE B:86 (π-Alkyl); GLY B:89 (Conventional H Bond); LEU B:91 (π-σ)

All studied structures (**1**–**10**) can form complexes with PDF from E. coli, demonstrating moderate affinity with ΔG values in the range of -6.5 kcal/mol to -7.1 kcal/mol *(Table 10)*. The most energetically favorable complexes are formed by compounds **7** and **9** (ΔG = -7.1 kcal/mol). These molecules show a combination of hydrophobic π–alkyl interactions with ILE B:44, ILE B:86, LEU B:125 and LEU B:161, as well as electrostatic and π-cation contacts with ARG B:97 and GLU B:95, enabling efficient anchoring within the protein binding site. For compound **7**, additional stabilization is provided by amide-π stacking and a π–donor hydrogen bond with GLY B:89.

Compounds **6** and **8** (ΔG = -6.8 kcal/mol) demonstrate stable binding due to hydrophobic interactions with ILE B:44, ILE B:86 and LEU B:91, as well as a π-cation interaction with ARG B:97. For compound **6**, a halogen bond (F) with GLU B:42 was additionally observed, which may enhance complex stability.

Compounds **1**–**5** and **10** have slightly higher ΔG values (-6.5 kcal/mol to -6.7 kcal/mol). Their binding is mainly mediated by single hydrogen bonds (GLU B:87, GLY B:89, GLN B:96) and hydrophobic π-alkyl and π-σ contacts with ILE and LEU residues. For some complexes, energetically unfavorable positive-positive interactions with ARG B:97 were observed, which may partially reduce overall binding stability.

Model structures **1**–**10** effectively interact with the active site of anaplastic lymphoma kinase (ALK), forming stable complexes with ΔG values in the range of -7.9 kcal/mol to -9.0 kcal/mol *(Table 11)*. The most energetically favorable was the complex of compound **8** with ALK (ΔG = -9.0 kcal/mol).

Table 11. Molecular docking results for ALK

Compound	ΔG, kcal/mol	Amino acid contacts (residues; interaction type)
1	-8.1	ALA A:1148 (π-Alkyl); LEU A:1256 (π-Alkyl); ASP A:1203 (Attractive Charge); LEU A:1122 (π-σ)
2	-8.8	LYS A:1205 (π-Alkyl); LEU A:1256 (π-σ); ALA A:1148 (π-Alkyl); ASP A:1203 (attractive charge; π-Anion); LEU A:1122 (π-σ)
3	-7.9	LEU A:1196 (π-Alkyl); ALA A:1148 (π-Alkyl); LEU A:1256 (π-σ); ASP A:1203 (Attractive Charge; π-Anion; Carbon H bond); LEU A:1122 (π-Alkyl); VAL A:1130 (π-Alkyl)
4	-8.2	ALA A:1126 (π-Alkyl); ALA A:1148 (π-Alkyl); GLY A:1128 (C-H bond); VAL A:1130 (π-Alkyl); LEU A:1256 (π-σ); LEU A:1122 (π-σ)
5	-8.8	ARG A:1253 (Conventional H bond); ALA A:1148 (π-Alkyl); MET A:1199 (Conventional H bond); SER A:1206 (Conventional H bond); ASP A:1203 (Halogen (F)); ASP A:1270 (π-Anion; Attractive Charge); LEU A:1196 (π-Alkyl); LEU A:1256 (π-σ); LEU A:1122 (π-σ); VAL A:1130 (π-Alkyl)
6	-8.8	ARG A:1253 (π-Alkyl); LYS A:1205 (π-Alkyl); ASP A:1203 (π-Anion; Attractive Charge); ALA A:1148 (π-Alkyl); LEU A:1256 (π-σ); LEU A:1122 (π-σ); VAL A:1130 (π-Alkyl)
7	-8.7	LEU A:1196 (π-Alkyl); LYS A:1205 (π-Alkyl); LEU A:1256 (π-σ); ALA A:1148 (π-Alkyl); LEU A:1122 (π-σ); ASP A:1203 (π-Anion; Attractive Charge)
8	-9.0	GLU A:1197 (Conventional H bond); LEU A:1256 (π-σ); ALA A:1148 (π-Alkyl); ASP A:1203 (π-Anion; Attractive Charge); LEU A:1122 (π-σ); LYS A:1205 (π-Alkyl)
9	-8.5	ASP A:1203 (π-Anion; Attractive Charge); ALA A:1148 (π-Alkyl); LEU A:1256 (π-σ); ARG A:1253 (π-Alkyl); LEU A:1122 (π-σ); VAL A:1130 (π-Alkyl)
10	-8.9	SER A:1206 (Conventional H bond); ALA A:1148 (π-Alkyl); ASP A:1203 (π-Anion; Attractive Charge); ARG A:1253 (Conventional H bond); LEU A:1256 (π-σ); LEU A:1122 (π-σ); LEU A:1196 (π-Alkyl)

High stability is associated with formation of a classical hydrogen bond with GLU A:1197, as well as electrostatic π-anion and charge-dependent interactions with ASP A:1203, a key residue in the kinase active site. Additional anchoring is provided by hydrophobic π–alkyl and π–σ contacts with ALA A:1148, LEU A:1122 and LEU A:1256, indicating efficient occupation of the hydrophobic pocket of ALK.

High affinity to ALK was also demonstrated by compounds **2**, **5**, **6** and **10** (ΔG = -8.8 kcal/mol to -8.9 kcal/mol). These molecules show a combination of electrostatic interactions with ASP A:1203 and ASP A:1270, hydrogen bonds with ARG A:1253, SER A:1206 and MET A:1199, and hydrophobic contacts with ALA A:1148, LEU A:1122, LEU A:1196 and VAL A:1130. For compound **5**, additional stabilization is provided by a halogen interaction (F) with ASP A:1203, which may positively influence inhibition selectivity.

Compound **7** (ΔG = -8.7 kcal/mol) forms a stable complex due to a π-anion interaction with ASP A:1203, π-alkyl contacts with LEU A:1196 and ALA A:1148, and hydrophobic interactions with LYS A:1205 and LEU A:1122, a typical binding profile for tyrosine kinase inhibitors. Compound **9** (ΔG = -8.5 kcal/mol) demonstrates a similar binding mechanism in the ALK active site, with dominance of electrostatic interactions with ASP A:1203 and hydrophobic contacts with ALA A:1148, LEU A:1256, LEU A:1122 and VAL A:1130. Compounds **1**, **3** and **4** have slightly lower binding energies (ΔG = -7.9 kcal/mol to -8.2 kcal/mol). Their interaction with ALK is mediated mainly by hydrophobic π-alkyl and π-σ contacts with ALA A:1148, LEU A:1122 and LEU A:1256. For compounds **1**, **4** and **10**, energetically unfavorable donor-donor interactions with MET A:1199 were observed; however, their negative impact is compensated by a substantial number of stabilizing hydrophobic and electrostatic contacts.

Discussion

The integrated SwissADME results indicate that the main factors that may limit the oral bioavailability of some derivatives are low aqueous solubility, increased polarity, and excessive lipophilicity. Compounds **2** and **5** show the most balanced pharmacokinetic profile, whereas for **6** and **7** the limiting factor is the combination of high lipophilicity with low solubility, and for **1**, **3**, **4**, **9** and **10** – excessive polarity, which may reduce membrane permeability.

Increased molecular weight, low Csp^3 fraction and high aromaticity may potentially impair solubility and transport across biological barriers. Excessive conformational flexibility of certain structures may also adversely affect "lead-like" characteristics. Low logS values indicate a risk of insufficient dissolution, and the predicted low absorption for compounds **7**, **9** and **10** suggests a need for structural or formulation optimization. Predicted P-gp substrate behavior (**1**, **3**, **4**, **8**) and potential CYP inhibition increase the risk of pharmacokinetic interactions. The lack of BBB permeation and absence of PAINS alerts are favorable features, although experimental validation remains necessary. The most promising for further studies are compounds **2**, **5** and **6**, while compound **1** fits the "lead-like" space and is reasonable as a starting structure for optimization. Overall, the series is suitable for rational lead optimization by adjusting polarity, lipophilicity, molecular weight, and flexibility, followed by experimental verification.

Molecular docking of the model series (**1**–**10**) demonstrated that all investigated molecules can form stable complexes with the active sites of the selected biological targets, as evidenced by negative binding free energies. The highest affinities were observed for CYP51 and COX-2, where ΔG values reached -11.0 kcal/mol and -10.2 kcal/mol, respective-

ly, indicating good structural complementarity of the ligands to the hydrophobic pockets of these enzymes.

For CYP51, hydrophobic and π–π interactions with aromatic residues, as well as hydrogen bonds with CYS A:394, play key roles in complex stabilization. Compounds **5**, **7**, **8** and **10** were identified as the most promising inhibitors. For COX-2, ligand binding is mediated mainly by interactions with ALA A:528, VAL A:350, GLY A:527 and TYR A:356; the lowest ΔG values are characteristic of compounds **4**, **6**, **7** and **9**. Docking to peptide deformylase from *S. aureus* (PDB: 1Q1Y) showed moderate but stable affinity of the investigated compounds (ΔG = -7.4 kcal/mol to -8.4 kcal/mol), with dominance of hydrophobic, π-π and hydrogen-bond interactions with residues VAL A:59, HIS A:154, SER A:57, TYR A:147, GLY A:58, ARG A:56 and GLU A:185. For ALK, key contributions come from electrostatic interactions with ASP A:1203 combined with hydrophobic contacts; the highest affinity was predicted for compounds **8** and **10**, while compounds **2**, **5** and **6** show close values.

In summary, compounds **5**, **6–8** and **10** exhibit the most pronounced multitarget profile, making them promising candidates for further experimental studies as potential pharmacologically active agents with a combined mechanism of action.

Conclusions

1. 3-((Indol-3-yl)methyl)-6-methyl-[1,2,4]triazolo[3,4-*b*][1,3,4]thiadiazine-7-carbohydrazide and its *N*′-arylidene carbohydrazides demonstrate the ability to form stable complexes with five biological targets (lanosterol 14α-demethylase, COX-2, PDF from *S. aureus*, PDF from *E. coli*, ALK), with the highest affinities observed for lanosterol 14α-demethylase, COX-2 and ALK.

2. The main factors that may limit oral bioavailability are low aqueous solubility, excessive polarity, and increased lipophilicity; the most balanced pharmacokinetic profile is predicted for compounds **2** and **5**.

3. From the perspective of multitarget activity and pharmacokinetic balance, the most promising are compounds **2**, **5–8** and **10**, making them candidates for further experimental studies and structural optimization.

Funding
The study was performed without financial support.

Conflicts of interest: authors have no conflict of interest to declare.
Конфлікт інтересів: відсутній.

Information about authors:
Fedotov S. O., Senior Lecturer of the Department of Toxicological and Inorganic Chemistry, Zaporizhzhia State Medical and Pharmaceutical University, Ukraine.
ORCID ID: 0000-0002-0421-5303
Hotsulia A. S., PhD, DSc, Professor of the Department of Toxicological and Inorganic Chemistry, Zaporizhzhia State Medical and Pharmaceutical University, Ukraine.
ORCID ID: 0000-0001-9696-221X

Відомості про авторів:
Федотов С. О., старший викладач каф. токсикологічної та неорганічної хімії, Запорізький державний медико-фармацевтичний університет, Україна.
Гоцуля А. С., д-р фарм. наук, професор каф. токсикологічної та неорганічної хімії, Запорізький державний медико-фармацевтичний університет, Україна.

Андрій Гоцуля (Andrii Hotsulia)
andrey.goculya@gmail.com

References
1. Burcevs A, Sebris A, Novosjolova I, Mishnev A, Turks M. Synthesis of Indole Derivatives via Aryl Triazole Ring-Opening and Subsequent Cyclization. Molecules. 2025;30(2):337. doi: 10.3390/molecules30020337
2. Sanapalli V, Sanapalli BK, Mohammed AA. Synthesis and Antibacterial Evaluation of an Indole Triazole Conjugate with In Silico Evidence of Allosteric Binding to Penicillin-Binding Protein 2a. Pharmaceutics. 2025;17(8):1013. doi: 10.3390/pharmaceutics17081013
3. Pravin NJ, Kavalapure RS, Alegaon SG, Gharge S, Ranade SD. Indoles as promising Therapeutics: A review of recent drug discovery efforts. Bioorg Chem. 2025;154:108092. doi: 10.1016/j.bioorg.2024.108092
4. Khan N, Furkhan MF, Ramasamy R, Malgija B, Thajudeen H, Ahamed VS. Coumarin-indole-triazole hybrids: Synthesis, antimicrobial evaluation, DFT insights, molecular docking, and dynamics as potential antibacterial agents. Chemistry Africa. 2025;8(8):3343-64. doi: 10.1007/s42250-025-01416-8
5. Shcherbyna R, Panasenko O, Polonets O, Nedorezaniuk N, Duchenko M. Synthesis, antimicrobial and antifungal activity of ylidenhydrazides of 2-((4-R-5-R_1-4H-1,2,4-triazol-3-yl)thio)acetaldehydes. Ankara Universitesi Eczacilik Fakultesi Dergisi. 2021;45(3):504-14. doi: 10.33483/jfpau.939418
6. Dovbnia DV, Kaplaushenko AH, Frolova YS. A study of hypoglycemic activity of acids and salts containing 1,2,4-triazole. Ceska Slov Farm. 2023;72:113-24. https://www.prolekare.cz/casopisy/ceska-slovenska-farmacie/2023-3-11/studium-hypoglykemickej-aktivity-kyselin-a-soli-obsahujucich-1-2-4-triazol-135087/
7. Karpenko Y, Hunchak Y, Gutyj B, Hunchak A, Parchenko M, Parchenko V. Advanced research for physico-chemical properties and parameters of toxicity piperazinium 2-((5-(furan-2-yl)-4-phenyl-4H-1,2,4-triazol-3-yl)thio)-acetate. ScienceRise: Pharmaceutical Science. 2022;(2):18-25. doi: 10.15587/2519-4852.2022.255848
8. Demchenko S, Lesyk R, Yadlovskyi O, Holota S, Yarmoluk S, Tsyhankov S, Demchenko A. Fused triazole-azepine hybrids as potential non-steroidal antiinflammatory agents. Scientia Pharmaceutica. 2023;91(2):26. doi: 10.3390/scipharm91020026
9. Safonov A. Method of synthesis novel N'-substituted 2-((5-(thiophen-2-ylmethyl)-4H-1,2,4-triazol-3-yl)thio)acetohydrazides. Journal of Faculty of Pharmacy of Ankara University. 2020;44(2):242-52. doi: 10.33483/jfpau.580011
10. Gotsulya A, Fedotov S, Zinych O, Trofimova T, Brytanova T. Synthesis and properties of S-alkyl 4-(4-chlorophenyl)-5-(pyrrole-2-yl)-1,2,4-triazole-3-thiol derivatives. Journal of Faculty of Pharmacy of Ankara University. 2023;47(3):1020-32. doi: 10.52794/hujpharm.1011368
11. Elrashedy A, Ibrahim NE, Abo-Salem H, Elaasser MM, El-Sawy ER. Design, synthesis, and molecular modeling of new 1,2,4-triazole-containing indole compounds as aromatase antagonists for the treatment of breast cancer. Bioorg Chem. 2025;163:108677. doi: 10.1016/j.bioorg.2025.108677
12. Mahmoud E, Abdelhamid D, Mohammed AF, Almarhoon ZM, Bräse S, Youssif BG, et al. Design, Synthesis, and Antiproliferative Activity of Novel Indole/1,2,4-Triazole Hybrids as Tubulin Polymerization Inhibitors. Pharmaceuticals (Basel). 2025;18(2):275. doi: 10.3390/ph18020275
13. Biovia. Discovery Studio Visualizer, v 19.1.0.18287 [Software]. 2019 [cited 2025 Sep19]. Available from: https://www.3ds.com/products/biovia
14. ChemAxon. MarvinSketch, Version 6.3.0 [Software]. 2015 [cited 2025 Sep19]. Available from: http://www.chemaxon.com
15. Worldwide Protein Data Bank. Protein Data Bank (PDB) [Database]. [cited 2025 Sep19]. Available from: http://www.pdb.org